RSC Advances

RSC Advances

ARTICLE

Intrinsic therapeutic and biocatalytic roles of ionic liquid mediated self-assembled platinum-phytase nanosphere

Sarvesh K Soni[a, ‡,*], Sampa Sarkar[a,b,‡], Selvakannan R. Periasamy[a], Dhiman Sarkar[b], Suresh K Bhargava[a*]

We herein report the inherent antitumor efficiency of the self-assembled phytase enzyme nanospheres and enhance its efficiency by decorating it with platinum nanoparticles and with an anticancer drug curcumin. Firstly, controlled self-assembly of phytase enzyme in an Ionic Liquid 1-butyl-3-methylimidazolium tetrafluoroborate [Bmim][BF$_4$], led to the formation of therapeutically active phytase nanosphere. These nanospheres were further decorated with platinum nanoparticles by adding the platinum ions to these spheres and the nanoparticles formation was mediated by specific interaction between the histidine residue (in active site of phytase enzymes) and the platinum ions and subsequent reduction of the ions into nanoparticles. The enzyme spheres act as functional soft template for the as-formed platinum nanoparticles. These Platinum decorated hybrid biomacromolecular phytase nanospheres were loaded with an anticancer drug curcumin and all different kind of nanospheres were subjected to *in vitro* cytotoxicity for their anticancer effect on three different kinds of cancer cell lines i.e. MCF-7, Hep-G2 and THP-1 derived human macrophages. We observed gradual increase in anticancer effect caused by only phytase nanosphere (25%), platinum-phytase nanosphere (37%), phytase-curcumin (78%) and platinum-phytase-curcumin nanosphere (90%) that establish this protein based system as a robust combinatorial drug delivery vehicle. The platinum-phytase spheres also proved its usability as a highly efficient green and reusable biocatalytic system for phytate degradation. The present work facilitates our understanding of ionic liquid based synthesis for multifunctional protein based drug delivery vehicles incorporating combinatorial chemotherapy for potential application as biopharmaceutical agents for tumor treatment and bio-catalysis.

1. Introduction

The design and fabrication of novel multifunctional drug delivery vehicles have received considerable attention in the last two decades especially those vehicles incorporate targeted drug delivery, biocompatibility, slow and sustained drug release profile. Among them, nano drug delivery vehicles are promising candidates due to their advantages that includes prolonged circulation time of the drugs[1], improved drug targeting and solubility, facilitate higher payloads and controlled release of the therapeutics into the blood stream or the targeted tumor tissues[2]. There are numerous approaches to synthesize nano drug delivery vehicles[3], among them self-assembly process[4], layer-by-layer technique (LbL)[5], mesoporous silica nanoparticles[6] and microfluidic devices[7] are the major methods to produce nanodrug delivery systems. Among the materials used for making nanodrug delivery platforms, polymer or other macromolecular based capsules have significant advantages over other fabricated inorganic drug delivery vehicles. Amphiphilic block-copolymers are the preferred materials to make nano drug delivery vehicles and self-assembling them in different solvent is the main approach to make these polymeric nanocapsules.

A major drawback in the afore-mentioned method is the capsules synthesized by these methods are biologically inert and can only be utilized for drug delivery application i.e. they don't have any intrinsic therapeutic value. Self-assembled materials of biological origin have superiority over above mentioned approaches and provide inspiration for the development of new materials for a variety of applications[8]. Due to the unique structural characteristic of proteins such as various functional groups, hydrophilic/hydrophobic domains and advantages such as natural metabolism in physiological systems and biocompatibility,[9,10,11] proteins can easily encapsulate various kinds of drug, food and nutrients in aqueous solutions, and can perform a central role as robust delivery vehicles[12, 13].

Recently, nanoparticle loaded protein drug carriers are considered as promising materials for cancer therapy[14, 15, 16]. Therapeutic proteins are the most preferred candidates among various FDA approved bio-pharmaceuticals[14, 17] because in comparison to small molecule/drugs, the specificity of protein-based treatment is unique. On the basis of their molecular type, therapeutic proteins can be grouped as

[a.] Centre for Advanced Materials and Industrial Chemistry, School of Applied Sciences, RMIT University, GPO Box 2476V, Melbourne, VIC, Australia, 3001.
[b.] Combichem Bioresource Centre, National Chemical Laboratory, Pune, India.
*E-mail: sarveshkumar.soni@rmit.edu.au ; Tel: +61 3 9925 2397
‡ Equal contribution
Electronic Supplementary Information (ESI) available: [Effect of varying concentrations of platinum salt, oleic acid, curcumin and ionic liquid on cell viability of HepG2, MCF-7 and THP-1]. See DOI: 10.1039/x0xx00000x

interleukins, interferons, hormones, growth factors, antibody based drugs and enzymes etc.[14]. Till now, different approaches for fabricating protein based nano-particles for food and drug delivery have been developed, including salt precipitation[18], desolvation[19, 20] and emulsion/solvent extraction[21]. However, most of the synthetic methods demand environmentally hazardous surfactants, organic solvents and very high salt concentration, which is not desirable in any biomedical application. Ionic liquids (ILs – commonly known as room temperature molten salts), very recently emerged as environmentally friendly reaction media, because of their unique physical and chemical properties[22], thus finding potential applications in every aspect of modern applied science, including biological sciences DNA transformation[23] and nanomaterials synthesis[24, 25]. Moreover the stability of enzymes/proteins has been proved to be increased in ILs over that in organic solvents[26]. All these advantages in combination with the green, designable properties make ionic liquids as promising candidates for enzyme encapsulation, immobilization and reusability studies[25]. This property of ILs in regards of bio-macromolecular self-assembly facilitated synthesis of organic-inorganic hybrid nanospheres can be explored to retain the functionality of organic component after incorporation of inorganic component, which is not a very regular phenomenon[27].

To the best of our knowledge the potential of ILs as reaction media for self-assembly of biomacromolecules (e.g. DNA, proteins or enzymes and peptides) to make functional nanospheres (made up of one type of enzyme units) for drug delivery applications has not been explored. The self-assembly of phytase enzyme (also known as myo-inositol hexakisphosphohydrolase)[28] in the IL 1-butyl-3-methylimidazolium tetrafluoroborate [Bmim][BF$_4$] leads to formation of functionally active phytase nanospheres. Addition of platinum ions to these spheres resulted in the formation of platinum nanoparticles on the surface of these nanospheres. In general, nanoparticles on the surface of any templating nanosphere require any reducing agent, surfactant, organic solvent, template core or emulsion phases but this method (see experimental section for more details), provides a straightforward approach to make Pt decorated enzyme nanospheres (hereafter referred as "Pt-Phy"). We recently have studied the self-assembling property of this kind of enzyme in ionic liquids and how it could act as functional template for synthesis of silica[29] and other inorganic metal nanospheres[30]. Interestingly, it was observed that phytase enzyme nanospheres retain their enzymatic activity and can be reused for multiple cycles.

Almost half of the therapeutic proteins that are approved by FDA or in clinical trials are glycosylated[31, 32] and phytase being highly glycosylated[33], attracted our interest to utilize it for drug delivery applications. Subsequently, we have demonstrated the drug loading capacity of these nanospheres by encapsulating a hydrophobic antitumor drug, curcumin (a diferuloylmethane, phytochemical compound present in Indian spice turmeric) and showed that these enzyme nanopsheres could have molecular level cavities that can load the antitumor drug like curcumin within its hydrophobic domains and releasing it. The FDA classifies, Turmeric as GRAS (Generally Recognized as Safe) and in this work we demonstrated, *in vitro* drug release and combinatorial anti-cancer effects of these nanospheres on three different cancer cell lines hepato cellular carcinoma (HepG2), breast cancer (MCF-7) (both adherent) and macrophase derived from the human monocytic leukemia cell ine THP-1. Interestingly all these three kinds of nanospheres showed capability to penetrate cell barriers. To this point, we envisage that self-assembled enzyme/protein nanospheres mimic like the cell penetrating peptides or a virus cage loaded with anti-cancer drug[34].

In this work, we present the self-assembled protein nanospheres (and their intrinsic anticancer property) that has the enzyme activity and further modified with platinum nanoparticles and curcumin, which render these enzyme nanospheres antitumor active. Ionic liquid mediated self-assembly of proteins and surface modification with antuitumor active agents can be developed as a therapeutic multifunctional drug delivery systems utilizing simple approach.

2. Experimental

2.1 Materials

Ionic liquid (IL) 1-butyl-3-methylimidazolium tetrafluoroborate ([Bmim][BF$_4$]) of electrochemical grade was purchased from Ionic Liquid Technologies (IoLiTec), Curcumin,, Potassium hexachloroplatinate (IV) (K$_2$PtCl$_6$), purchased from Sigma-Aldrich. Fetal bovine serum (FBS) and Minimum Essential Media (MEM) (without phenol red and with 2.5 mM L-glutamine) medium were purchased from GIBCO Biosciences. All other chemicals used were analytical grade. All chemicals were used as received, unless specified.

2.2 Phytase purification

Phytase was purified from submerged fermentation broth of fungus *Aspergillus niger* that was maintained on Potato Dextrose Agar (PDA) slants, as described previously[33, 35]. In this particular report[33] 2 kind of phytases (I and II) were reported and we used Phytase I for the current studies.

2.3 Ionic liquid-mediated synthesis

2.3.1 Phytase nanospheres

A typical synthesis reaction of phytase nanospheres in ILs was performed in 0.5 mL volume containing 490 µL of the IL [Bmim][BF$_4$] and 10 µL of purified phytase enzyme (1 mg mL^{-1} dissolved in water), thus achieving a final enzyme concentration of 20 µg mL^{-1} in the reaction. The IL-phytase mixture was incubated at 37 ± 0.1 °C for 24 h with gentle reciprocal shaking, after which samples were centrifuged at 8,000 rpm followed by washing with deionized water and acetonitrile to remove the viscous ionic liquid. Phytase nanospheres thus obtained were further analyzed by TEM.

2.3.2 Ionic liquid-mediated synthesis of Platinum nanospheres

ARTICLE

10 mM Potassium hexachloroplatinate (IV) [K_2PtCl_6] solution in MQ water was used as stock solution and diluted further with the mixture containing IL and phytase nanospheres. to obtain stable platinum nanoparticles in polar media. 10 μL of K_2PtCl_6 stock solution (10 mM) in water was added to 500 μL of the aforementioned reaction mixture containing IL and phytase nanospheres. The final reaction volume was maintained at 1 mL after addition of 490 μL of respective Ionic Liquid. The 1 mL reaction contents were incubated at 37 ± 0.1 °C for 24 h under stirring conditions, during which all the reactions involving phytase became turbid, indicating K_2PtCl_6 reduction (Figure 1). After 24 h of reaction, samples were centrifuged at 8,000 rpm followed by washing with deionized water and acetonitrile to remove the viscous ionic liquid. Higher concentration of K_2PtCl_6 was also used and this reaction didn't lead to synthesis of phy-pt nanospheres probably due to competitive interaction between the IL cation and hexachloroplatinate anion and the resultant precipitation of their mixture. Platinum nanostructures thus obtained were further analyzed by TEM and used for enzyme reusability studies. In a control experiment, 10 μL of deionized water was added to 10 μL of K_2PtCl_6 stock solution and 980 μL IL, and the reaction was pursued along with the main experiment. However, no turbidity was observed in the control reaction containing water, thereby negating the possibility of water-mediated reduction of K_2PtCl_6 in IL [Bmim][BF_4] and suggesting the role of phytase towards K_2PtCl_6 reduction in ILs. Washing the reaction products with deionized water at 37 °C (instead of washing with acetonitrile) did not show any significant difference in Platinum nanoparticles formed, however samples not washed with acetonitrile were difficult to image in TEM due to residual presence of ILs in those samples. The TEM images shown in this work obtained from the nanoparticles samples that were washed with acetonitrile.

2.4 Enzyme activity assay and reusability assay

To determine the enzymatic stability of phytase in hollow Platinum nanospheres after encapsulation, synthesized using 20 μg mL^{-1} phytase in IL [Bmim][BF_4] were dispersed in 1 mL of Gly-HCl buffer (100mM, pH 2.5). 100 μl of hollow platinum nanoparticles in Gly-HCl buffer were mixed with 300 μL of Gly-HCl buffer and 100 μl of enzyme substrate (phytic acid, 15 mM, pH 2.5) was added to the reaction. The reaction mixture was then incubated at 55 °C for 30 min at 300 rpm, followed by centrifugation to obtain a clear supernatant and nanoparticles pellet. The inorganic phosphorus released from phytic acid due to enzyme activity was determined in supernatant by a modified ammonium molybdate phytase activity assay[36]. The experiment was continued for 8 cycles and the enzymatic activity obtained in first cycle was considered as 100% to compare with subsequent cycles. Experiments were conducted in triplicates to minimize experimental error.

2.5 Preparation of Platinum-Phytase-Curcumin and Phytase-curcumin Nano-spheres

Pt-Phy spheres and self-assembled phytase spheres were dispersed in phosphate buffer (pH ≈ 7.2), centrifuged and the

supernatant was removed. The pellet was re-dispersed in ethanol (0.5 mL) and centrifuged at 14,500 g for 10 min. This procedure was repeated. The resulting pellet containing Platinum nanospheres were dispersed with drug/oleic acid (oleic acid is FDA approved for drug delivery applications) (0.1 mL, 0.1mg mL^{-1}), and the mixture was incubated for 24 h at 25 °C. The Curcumin/oleic acid loaded Pt-Phy nanospheres and Phytase spheres were centrifuged (14,500 g) for 10 min and washed two times with 15% ethanol to remove excess drug/oleic acid from the nanosphere walls. To determine the amount of curcumin loaded onto the Pt-Phy nanocontainers, we examined the spheres by UV–Vis spectrophotometry. The Curcumin/oleic acid-loaded Platinum spheres were then exposed to ethanol to dissolve the curcumin and the curcumin absorbance in the supernatant was measured. Using a UV–Vis absorbance calibration curve, we calculated that curcumin loading was 10ng/μg of protein sphere.

2.6 Cell culture and maintenance

Human acute monocytes THP-1, Hepato cellular carcinoma HepG2 and breast cancer MCF-7 cell lines were obtained from National Centre for Cell Science (NCCS) (Pune, India). Cell lines were routinely maintained in MEM (without phenol red) medium supplemented with 10% heat-inactivated FBS at 37 °C, 5% CO_2 and 95% in 75 cm^2 tissue culture flasks.

2.7 Conversion of THP-1 monocyte into macrophage

THP-1 monocyte cells (1 × 10^4 cells/mL) were grown in a 96-well containing 100 μL MEM medium at pH 7.4 at 37 °C for 4 days at 5% CO_2 and 95% relative humidity to reach the required cell density (5 × 10^4 cells/mL) followed by treatment with 100 nM of phorbol myristate acetate (PMA)[37]. The culture was then incubated for a further 24 h to allow macrophage conversion in the plate. After that cells were washed 3-4 times with PBS to remove the non - macrophage cells (1-2%) from the wells and the cell culture was filled with 100 μL MEM medium as mentioned earlier.

2.8 Cell proliferation assay

Cell proliferation was monitored by following an earlier described method[38]. Briefly, 100μl of THP-1-derived human macrophage, HepG2 and MCF-7 cells were seeded in a 96 well plate with a density of 2x10^{5}cells/ml. Samples (5 μl) were added in the plate just after adding the cells in the wells and incubated 5 days for THP-1 derived human macrophages, 3 days for HepG2 and 7 days for MCF-7 respectively at 37 °C in presence of 5% CO_2 and 95% humidity within the incubator. After incubation, 10 μl of MTT solution (5mg/ml) was added to each well and incubated for 1hr in the CO_2 incubator. At the end of this period, 200 μl of acidified isopropanol was added in each well and plate was incubated for another 4 hrs to solubilize the purple formazan crystals produced. Then, the absorbance was measured at 490 nm with SPECTRA max PLUS.

As positive controls cells were incubated without test samples and as a vehicle (negative control) only media with respective

RSC Advances Accepted Manuscript

sample solvent were added. All the samples were taken in triplicates.

2.9 Live-dead stain

Adherent HepG2, MCF-7 and THP-1 derived human macrophage cells (1×10^5) were incubated on the cover slips with RPMI 1640 medium supplemented with 10% FBS at 37 °C, 5% CO_2 and 95 % humidity. After 24 h incubation 2.5µl of curcumin /oleic acid –loaded spheres were added to the culture medium and keep it for 24h. Coverslips with nanosphere loaded adherent cells were fixed with 4% Para formaldehyde and stain with freshly prepared staining solution Propidium iodide (PI) and Hoechst dye for 30 min. Live cells can be detected by Hoechst which can entered into the cell and dead cells can be detected by PI which is not permeable to the cells. Fixed cells were washed thoroughly in PBS (2-3 times) before being mounted in a drop of glycerol (70%) on a glass slide.

2.10 Materials Characterization

TEM imaging of nanospheres was performed using the 100 kV JEOL 1010 TEM instrument after drop casting the solutions containing nanospheres on a Cu TEM grid. XRD measurements were performed using Cu Kα radiation in a General Area Detector Diffraction System (GAADS) Bruker AXS D-8 Discover. XPS measurements of Platinum-Phytase nanospheres were carried out on a Thermo K-Alpha XPS instrument at a pressure better than 1×10^{-9} Torr (1 Torr = 1.333×10^2 Pa). The general scan and Au 4f, Ag 3d, Pd 3d, and Ni 2p, core level spectra from the respective samples were recorded with unmonochromatized Aluminium Kα radiation (photon energy = 1486.6 eV) at a pass energy of 50 eV and electron takeoff angle (angle between electron emission direction and surface plane) of 90°. The core level binding energies (BEs) were aligned with the adventitious carbon binding energy of 285 eV. Inductively coupled plasma mass spectrometry (ICP-MS) studies of these materials were carried out using the Agilent 7700 ICP-MS instrument.

3. Results and discussion

3.1 Synthesis of Platinum nanoparticles functionalized Enzyme Nanospheres

The self-assembled phytase nanospheres obtained in IL [Bmim][BF$_4$] were utilized as catalytic template for the in-situ synthesis of platinum nanoparticles decorated enzyme spheres (hereafter mentioned as Pt-Phy). To obtain the Pt-Phy nanospheres, aqueous solution of potassium hexachloroplatinate (K$_2$PtCl$_6$) was mixed with IL [Bmim][BF$_4$] containing phytase nanospheres (pre-assembled). Optical image of the as-synthesized phytase nanospheres and Pt-Phy nanospheres in aqueous solution are illustrated as Figure 1 and change in color of white enzyme spheres to dark brown indicated the formation of platinum nanoparticles on the surface of enzyme nanospheres.

Transmission electron microscopy (TEM) image of phytase nanospheres, obtained after phytase enzyme self-assembly in
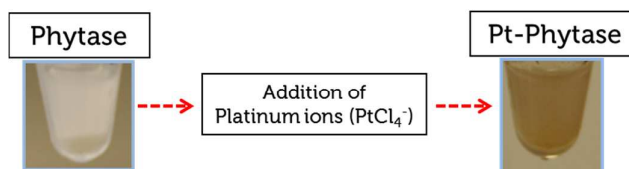

Figure 1. Photographic image of self-assembled phytase and Platinum-Phy nanospheres in ionic liquid [Bmim][BF$_4$].

the IL [Bmim][BF$_4$] has been shown as Figure 2A. Since the protein spheres were unstained, exposure to high energy electron beam tends to break the protein aggregates to char and burst. Illustrated in Figure 2B-D are the TEM images of Pt-Phy nanospheres synthesized in [Bmim][BF$_4$]. The diameter of these Pt-phy nanospheres ranges from 200 nm to 300 nm and
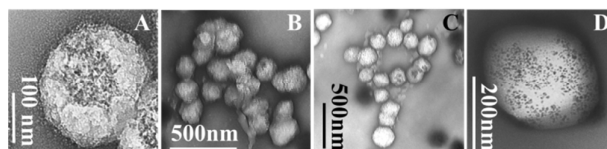

Figure 2. Self-assembled Phytase Enzyme Nanospheres in Ionic Liquid [Bmim][BF$_4$] as Templating Nanoreactors for platinum nanospheres (A) higher magnification TEM images of self-assembled phytase (20 µg mL^{-1}) nanospheres synthesized in ionic liquid [Bmim][BF$_4$] (B) TEM images of platinum nanospheres synthesized in ionic liquid [Bmim][BF$_4$] using self-assembled phytase nanospheres as catalytic templates (C) Platinum-Phy nanospheres after exposure to electron beam (D) Higher magnification image showing Platinum nanoparticles (~5.0 nm) on the surface.

have quasi-spherical morphology with the rough surface. Platinum nanoparticles on the surface of enzyme spheres were uniform in size (~5 nm diameter) and clearly visible on the surface of self-assembled phytase nanosphere in Figure 2D. The particles were unevenly distributed on the surface of enzyme nanosphere and some areas on the Pt-Phy nanosphere surface seen with very less population of particles. A precipitate of salt ([Bmim]$_2$[PtCl$_6$]), dark brown in color was formed in a control experiment (without any enzyme molecules) when [Bmim][BF$_4$] was allowed to react with K$_2$PtCl$_6$ (shown as Figure 3) in reaction.
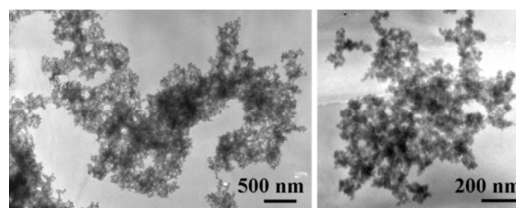

Figure 3. TEM images of precipitated salt (synthesized in ionic liquid [Bmim][BF$_4$] without enzyme molecules. (Control (K$_2$PtCl$_6$ + [Bmim][BF$_4$])).

The self-assembly of phytase enzyme in IL [Bmim][BF$_4$] resulted in the development of enzyme nanospheres and using them as templates for the synthesis of platinum nanoparticles,

which is a unique approach to make multifunctional enzyme spheres containing nanomaterial in an ionic liquid. It is interesting to observe the formation of Pt-Phy nanospheres in the absence of any external reducing agent, suggesting that self-assembled phytase molecules can enzymatically reduce potassium hexachloroplatinate, and also acted as a template for the as-formed platinum nanoparticles to form Pt-Phy. Phytases (isolated and purified to homogeneity from fungus *A. niger*) used in this study belongs to Histidine Acid Phosphatase sub-class and share a catalytically active site motif Arg-His-Gly-X-Arg-X-Pro (RHGXRXP), wherein the histidine (highly catalytic) residue is responsible for the hydrolysis of phytic acid substrate[39]. 7.1% of total amino acids in phytase enzyme are basic amino acids (Lys, Arg, His)[33] and these amino acids were already known for the reduction of noble metal ions into their nanoparticles[40, 41]. Therefore histidine in the active site and basic amino acids present on the surface of phytase nanospheres were attributed for reduction of platinum ions and resulted in the formation of platinum nanoparticles on its surface.

Studies on the fabrication of metallised protein nanofilaments also indicate that histidine residues are the most preferred sites for Platinum (II) binding[40] and metal cations' binding on organic surface suggest to lowering the interfacial energy associated with nucleation of inorganic moiety.

3.2 Application as combinatorial drug delivery agent *in vitro*

The application of protein nanoparticles as drug carriers has recently engrossed so much attention because of biocompatibility and easy to degrade by biological system (due to the highly reducing environment and presence of higher concentration of proteases in lysosome). The advantage of using protein sphere is that it provides lots of chemical functionalities on its surface (amine and carboxylic acid residues) and hydrophobic inner chambers. The molecular level voids/cavities of self-assembled Pt-Phy nanospheres were utilized to load a hydrophobic anticancer drug curcumin that exhibits anti-oxidative and anti-inflammatory properties and can induct apoptosis and suppress the formation of procarcinogens by various kinds of mechanism[42].

3.2.1 Anticancer effect of Pt-Phy-Curcumin nanospheres

Effect of Pt-Phy-Curcumin nanospheres (hereafter mentioned as S-5) was observed qualitatively on three cancer cell lines Hepatocellular carcinoma, human (HepG2) (Figure 4a), Michigan Cancer Foundation – 7 (MCF-7) breast cancer cell line (Figure 4b) and THP-1 macrophage derived from human acute monocytic leukemia cell line (THP-1) (Figure 4c) through Hoechst/propidium iodide (live/dead) staining.

In parallel we performed another, independent assay to quantify cytotoxicity via MTT cell viability assay. Along with S-5, Phytase in Mili Q Water (hereafter mentioned as S-1), Self-
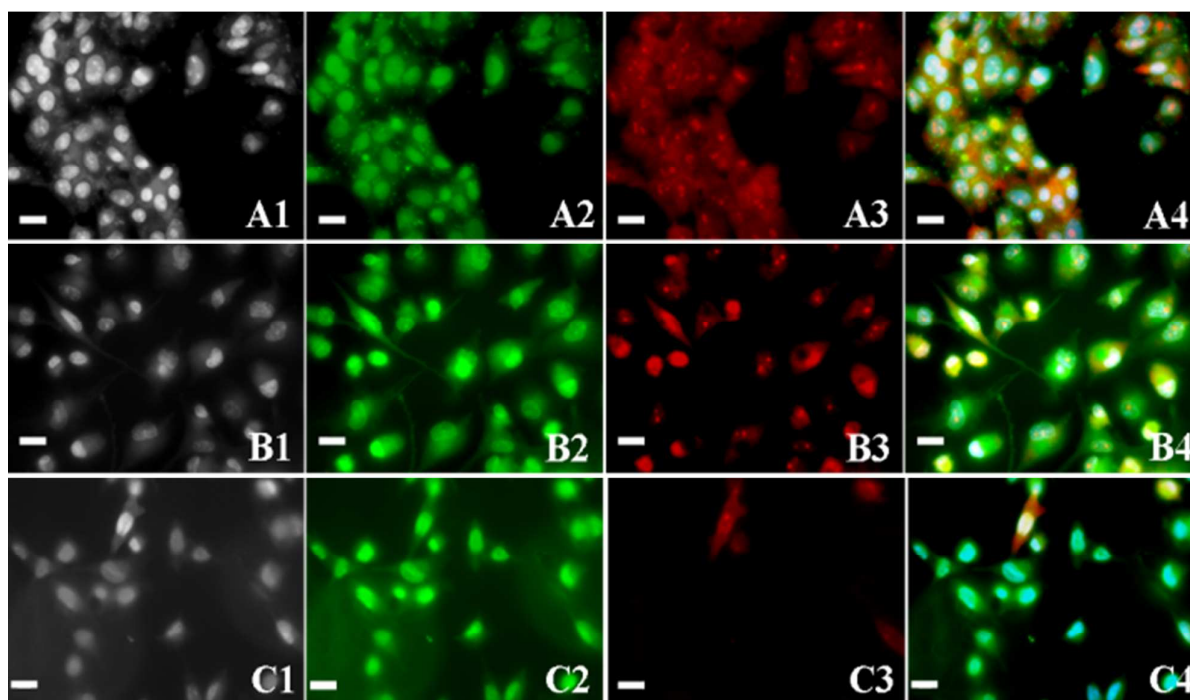

Figure 4. Phase contrasts Fluorescence microscopy images (20X Objective) of the uptake of curcumin loaded Platinum-Phy nanospheres by Hep-G2 (A1-A4), MCF-7 (B1-B4), THP-1 macrophage(C1-C4) Cells. The images show Bright field image (Both Live and Dead cells) (A1, B1, C1), the fluorescent signal arising from curcumin (A2, B2, C2), Propidium Iodide dye (A3, B3, C3) and merged images of curcumin and Hoechst/propidium Iodide (live /dead stain) (A4, B4, C4). The scale bars correspond to 20 μm.

for cancer therapeutics

assembled Phytase nanospheres (hereafter mentioned as S-2),

Pt-Phy (hereafter mentioned as S-3), Phy-curcumin (hereafter mentioned as S-4) were also tested for their cytotoxicity on all three cell lines (Figure 5). Observed Cytotoxicity of S-5 (containing 100ng curcumin/10μg of protein spheres, equivalent to .54 μM of curcumin) on HepG2 and MCF-7 85% and 75 % respectively was very high in comparison to THP-1 macrophage cell line (30%). The same trend was followed and observed in all the cytotoxicity experiments i.e. Figures 4, 5 and figure in supplementary information S1, S2, S3, S4 and S5.

There are reports in literature those have investigated the cytotoxicity of curcumin on THP-1 monocytic cells[43][47], however it is associated with very high concentrations of curcumin ((12.5–25 μM), in present case it is 0.54 μM (moreover it might be associated with the concentration of intracellular proteolytic enzymes and pH of THP-1 macrophage cells. Due to this the curcumin/protein sphere might have been degraded in phagosome, hence less cytotoxicity was observed

Uptake of curcumin-oleic acid-loaded platinum nano spheres by HepG2, MCF-7 and THP-1 cancer cell was investigated (1ng curcumin/100ng of protein or .54 μM curcumin for $2x10^4$cells) and visualized using phase contrast fluorescence microscopy after 24 hrs of incubation at 37 °C (Figure 4A, 4B and 4C). In Figure 4A1, 4B1 and 4C1 we have showed the bright field image (including both live and dead cells) of all three cell lines HepG2, MCF7 and THP-1 respectively, Figure 4A2, 4B2 and 4C2 clearly revealed the interaction of Pt-Phy-curcumin nanospheres to all three cell lines that is clearly evident by green fluorescence emission due to the curcumin from all the cells. Figure 4A3, 4B3 and 4C3 indicates the red fluorescence arising from the dead cells because of PI. PI is a nucleic acid (both DNA and RNA) stain and can also intercalate into free cytoplasmic RNA and due to this reason, in Fig. 4A3, 4B3 and 4C3 few dead cells' cytoplasm is showing light red stain, however most of the dead cells are with dark red nucleus. Moreover the possibility of stained DNA to leach out from nucleus of dead cells to cytoplasm also can't be ignored. Figure 4A4, 4B4 and 4C4 are the superimposed image of cells that confirm the same area of cells were imaged and blue fluorescence was arising (in Figure 4C4) due to Hoechst dye which indicated most of the cells were live. However there was no blue fluorescence detected in case of Figure 4 A4 and Figure 4 B4 that proved cytotoxic effect exerted by Pt-Phy-Curcumin nanospheres.

These images matches well with our MTT cell viability assay results (Figure 5-S5) and indicated a specific cytotoxicity on HepG2 and MCF7 cells (as most of the cells those internalize the curcumin were dead) but substantially low on THP-1 derived human macrophages.

3.2.2 Combinatorial anticancer effect of phytase, platinum-Phytase, phytase-curcumin and platinum-phytase-curcumin nanospheres

As shown in Figure 5, Self-assembled phytase nanospheres exerted 23 % Cytotoxicity on HepG2 cells that is . ~ 13 % less

in comparision to cytotoxicity exerted by same concentration of phytase enzyme molecules in solution. This phenomenon can be associated to ~10-15 % loss in native enzyme activity of phytase while self-assembling process to make nano-spheres of it in ionic liquid.

The reason to choose Phytase (Phosphohydrolase) as a model enzyme is because of its intrinsic property to enzymatically
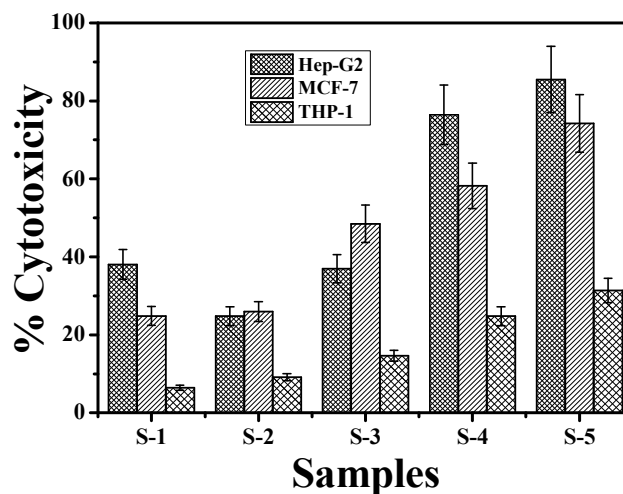

Figure 5. MTT cell proliferation and viability assay showing the percentage cytotoxicity of purified Phytase in D/W (S-1), Self assembled phytase nanospheres synthesized in Ionic Liquid [BMIM][BF$_4$] (S-2), Self assembled Pt-Phy nano spheres in Ionic Liquid [BMIM][BF$_4$] (S-3), Self-assembled Phytase spheres loaded with curcumin (S-4), Platinum-Phy nanospheres loaded with curcumin (S-5) on HepG2 , MCF-7 and THP-1 macrophase cells. 5 μl of sample (S1-S5) (protein concentration 20μg/ml) was used for $2x10^4$ cancer cells.

cleave the protruding phosphate groups from the phospholipids bilayer membrane of the cancer cell lines[44, 45] and leading to disintegration of cell membrane and killing of cancer cells. It was observed that after loading of platinum nanoparticles, the same amount of particles exert 37% cytotoxicity. Loading of curcumin made Pt-Phy spheres 53% more cytotoxic and overall cytotoxicity expressed by Pt-Phy-Curcumin particles was ~90%. It is interesting to note that addition of curcumin to Phytase nanosphere exerted ~78% of cytotoxicity. A sequential increase in cytotoxicity of nanosphere with platinum and curcumin proves this system to be a tool for combinatorial drug delivery. This phenomenon of sequential enhancement in cytotoxicity on HepG2 is also presented as Scheme 1.

The Pt-Phy-Curcumin nanospheres were washed with 15% ethanol (see material and methods) and no platinum ions were detected in supernatant, it suggests that the similar amount of platinum was present in protein spheres loaded with curcumin for anticancer activity. When pt-phy-curcumin nanoparticles were tested *in vitro* (in PBS buffer pH 7.2 at 37 °C) for release of curcumin and platinum nanoparticles from protein spheres, 4-5 % of curcumin (tested by dissolving the supernatant in ethanol and quantified by spectrophotometer) and 3-4% of

total platinum ion release was observed (checked in supernatant by ICPMS), after 48 hours of incubation.
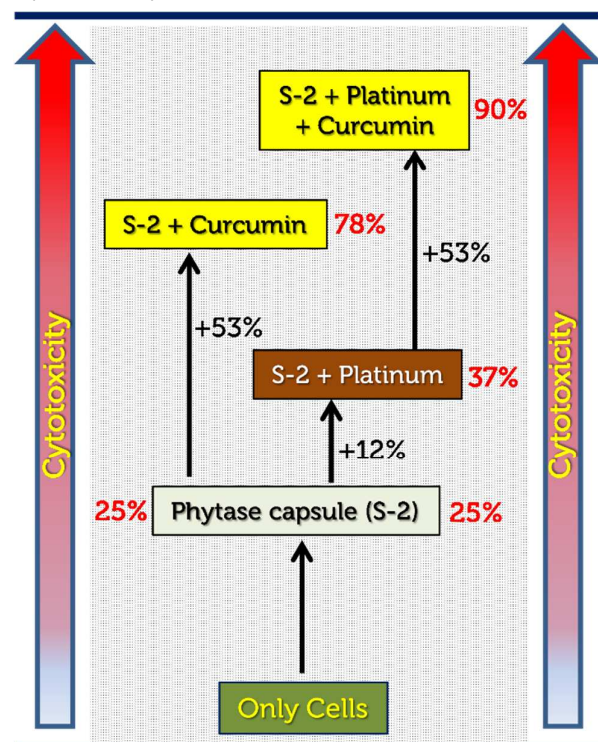
Scheme 1. Schematic illustration of combinatorial cytotoxicity by self-assembled nanospheres. When cancer cells were treated with only phytase nanospheres it confer 25% cytotoxicity and after addition of platinum and curcumin to this system cytotoxicity enhanced to 37 and 90%, respectively.

Effect of various concentrations of K_2PtCl_6, Oleic acid, curcumin dissolved in Oleic acid and deionized water, and different concentrations of Ionic liquid [Bmim][BF$_4$] in deionized water on HepG2, MCF-7 and THP-1 derived human macrophage cells are shown in supplementary information as Figure S1, S2, S3, S4 and S5, respectively (as cytotoxicity control experiments). From these results, it has been observed that, interestingly 1000 ng of free curcumin didn't give even the similar cytotoxicity, as compared to the cytotoxicity caused by 1ng of curcumin loaded on protein nanospheres (Figure 5). This might be because of nanosized protein spheres, those were able to protect the extraceullar degradation of curcumin, as well as increase its uptake by permeating within the lipidic cell membrane and release curcumin inside the cancer cells.

Due to the property of developing drug resistance in tumor cells, chemotherapy via small-drug molecules (the use of single anticancer agent) fails to achieve complete reduction in cancer[46]. So that most of the clinical procedures tend to use combination of anticancer agents[47]. Cisplatin and anthracycline based topoisomerase II (TOP2)-inhibitors[48] are the most commonly used chemotherapeutic agents those have been explored successfully against *in vitro* and *in vivo* lung cancer models as combination chemotherapy. It

emphasizes the potential of drug combination (pt-Phy-cur) used in this study, for killing the cancer cells. These studies represent examples of drug synergism where the co-administered two drugs lead to significantly greater activity than predicted from the simple addition of the effects of each drug component[49]. Combinatorial approaches also have been shown to improve the therapeutic efficacy of toxic drugs via enhanced permeation and retention (EPR) effect[50] and help to protect drugs from premature degradation and clearing from the system.

Pt-Phy-Curcumin delivered two type of anticancer agents in a single nano sphere, potentially giving rise to enhanced cytotoxicity in comparison to the free drug (Figures 4, S3 and S4) and the dose requirement for tumor treatment can be lowered to reduce toxicity arising due to dose-limiting and increase anti-cancer activity. The size of the particles/spheres (<300 nm) studied here is within the range reported to utilize the selectively permeable nature of tumor blood vessels[51]. It is noticeable that these *in vitro* experiments were performed under non-reducing conditions, however, it is expected that Pt-Phy-curcumin spheres will go under disassembly in reducing environments in the lysosomal compartments of the tumors via cleaving of the disulfide bond present in phytase (that is made up of 2 homo-dimers) – curcumin complex.

3.3 Characterization of the Phy and Pt-Phy nanospheres

In order to elucidate the nature of crystalline phase during the platinum nanoparticles formation on self-assembled phytase spheres in ionic liquid, the XRD patterns of Pt-Phy nanospheres was studied using General Area Detector Diffraction System (GADDS) and the results are presented as Figure 6.

Since gold coated silicon wafer was used as substrate to obtain the XRD pattern of Pt-Phy nanospheres, the diffraction peaks
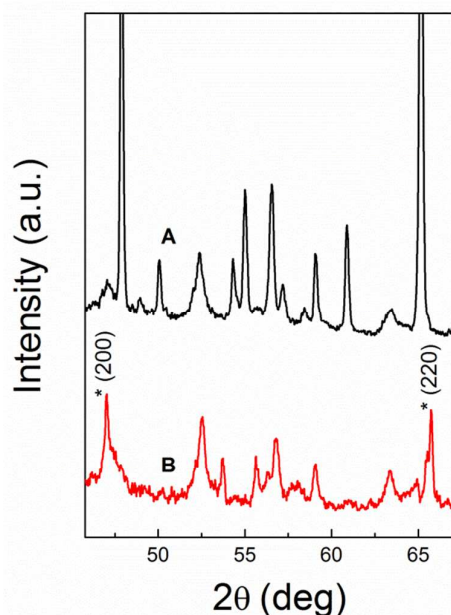

Figure 6. X Ray diffraction pattern obtained from self-assembled Phytase (A) and Platinum-Phy nanospheres (B) in ionic liquid [Bmim][BF$_4$]. * Peaks correspond to platinum metal crystal planes (200) and (220), other peaks are originating from the crystalline phytase template.

correspond to the different crystalline planes of polycrystalline gold were also observed at 38.2°, 44.5°, 64.7°, (crystal planes (220), 77.75° of PCPDF data base no. (004-0784). It is clearly seen that XRD bragg reflections observed at 46.96° and 66.94° were attributed to the (200) and (220) crystal planes of metallic platinum corresponds to PCPDF data base no. (00-004-0802). Some additional peaks were also observed, which might be due to the crystalline nature of enzyme spheres those were formed during the self-assembling process of phytase in IL. The crystallinity of phytase nanospheres is an interesting avenue for separate structural biology research however it is way beyond of the scope of current study so that it has not been explored further. A single step synthesis of crystalline phytase nanospheres on room temperature , envisage that ionic liquids could play an incredible role in enhancement of crystallinity of protein/biomaterials based nano drug delivery systems and that would lead to synthesize stable and sturdy protein nanospheres . In order to understand the chemical state of platinum in Pt-Phy nanospheres, XPS study of this material was carried out and the results are presented as Figure 7.

The presence of Pt 4f7/2 core level binding energies observed at 73 eV clearly indicating the presence of platinum on the surface of these spheres. This is a clear indication of platinum nanoparticles formation on the surface of phytase nanospheres. The Pt 4f core level for tetravalent platinum
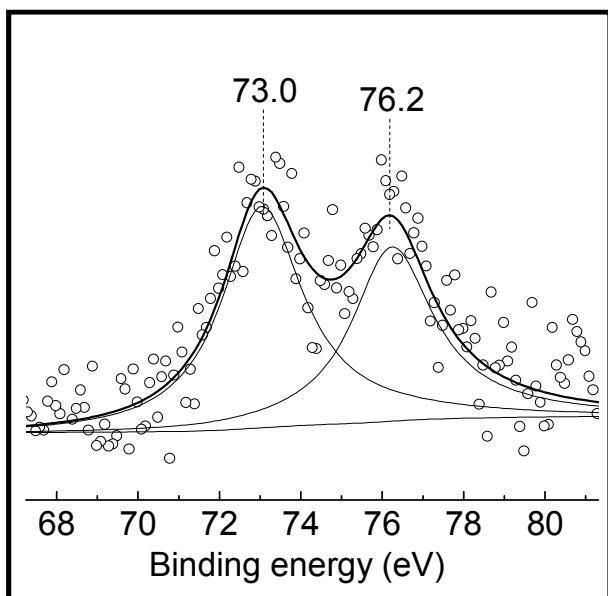

Figure 7. XPS core level spectra recorded from Platinum-Phy nanospheres (4f 7/2 and 4f 5/2) film deposited on a Si (111) substrate by drop-coating. The solid lines are nonlinear least-squares fits to the data.

(used here as platinum precursor) binding energy usually appeared around 75.5 eV, and in the present case it decreased to 73 eV. This result clearly reveals that the reduction of platinum ions occurred and it might be due to the interaction of platinum salt with the phytase nanospheres.

These results witnessing the fact that platinum ions were reduced on the surface of phytase spheres and the resulting platinum nanoparticles assembled on the template of phytase nanospheres. Earlier reports have shown that phytase was known to reduce noble metal ions such as gold and silver ions into their respective nanoparticles[36], thus the reducing ability of phytase was responsible for the reduction of platinum ions. Mediating the platinum nanoparticles formation and the assembly of the as-formed particles onto the soft template clearly witness the multifunctional role of phytase enzyme. Amount of platinum metal deposited onto nanospheres was estimated by the inductively coupled plasma mass spectrometry (ICP-MS) analysis of Pt–Phy spheres and Pt-Phy-Curcumin and concentrated nitric acid was used to digest it. Pt-Phy sphere consumed 63% of platinum ions from the total amount of metal ion (.1 mM in the parent solution) used during the reaction. Interestingly the Pt-Phy nanospheres could hold ~34 µM of metal per µg of protein, it is significantly 10-fold more than gold and silver, however close to palladium[30], it may be assigned to imidazolium groups' (present in histidine moieties of phytase enzyme) higher binding ability to platinum family metal ions including platinum. When Pt ions were incubated in the histidine rich peptide nanotube Pt ions bound carboxylate oxygens of histidine and subsequent reduction of the complexes produced Pt nanocrystals on the peptide nanotubes[41]. The similar mechanism might be suggested for reduced Pt nanocrystals on the surface of self-assembled protein nanospheres in the present case.

3.4 Biocatalytic applications of Pt-Phy nanospheres and their re-usability studies

Reusable biocatalysts and peptide loaded nano-vehicles[52] have attracted lots of attention due to their widespread applications in therapeutics, it emphasizes the immobilization of
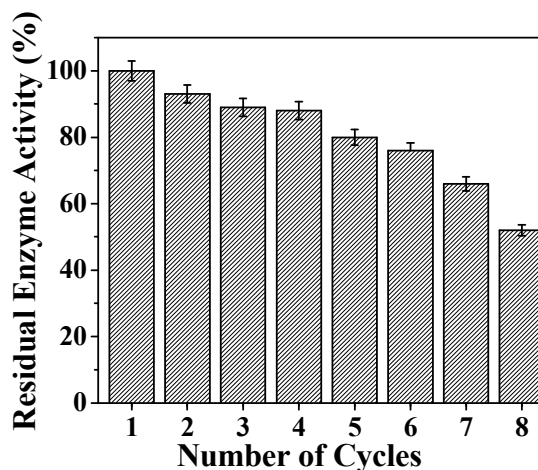

Figure 8. Reusability study of phytase enzyme (20 µg mL^{-1}) in situ encapsulated within Platinum-Phy nanospheres during their synthesis in ionic liquid [Bmim][BF$_4$].

industrially relevant enzymes onto solid supports as an

ARTICLE

extensive research area. However, the major challengeassociated with the enzyme immobilization strategies is the retention of enzyme activity onto a reusable substrate and unique solvent properties of ILs[26] also suggest its use to preserve the enzyme activity. Since self-assembled phytase nanospheres act as a template for growth (*in situ*) of platinum nano particles in IL, there is a high possibility that enzyme molecules are entrapped within the platinum nanostructure (Pt-Phy nanospheres in [Bmim][BF$_4$]) during their synthesis. Therefore, Pt-Phy nanospheres synthesized in IL were tested for reusability of enzyme (Figure 8).

When phytase activity was tested (see experimental section for details), pt-phy nanospheres formed in [Bmim][BF$_4$] were found to express substantial enzyme activity (a loss in 18-25% activity was also observed while the self-assembling process of native enzyme molecules and further platinum nanospheres in ionic liquid) that was retained for at least up to six cycles (Figure 8) and ~ 60% activity was retained (of self-assembled Pt-Phy and 49-45 % of native enzyme in aqueous solution) after 8 cycles.

The reusability studies of phytase nanospheres showed that these nanospheres kept their enzyme activity only up to 3 cycles and the activity significantly dropped to 50% and further in the successive cycles. In comparison, Pt-Phytase nanospheres can be reused for many times, wherein the

enzyme stability and the functionality can be retained due to the structural rigidity and compactness provided by the platinum nanoparticles.

The enzyme activity is highly sensitive to factors of external surrounding such as solvents, pH and temperature, and a small change to these factors leads to conformational change and ultimately loss in activity, however it is particularly very interesting that phytase activity in Pt-Phy nanospheres was retained. So the advantages of utilizing self-assembled phytase nanospheres over existing approaches include less time consuming synthesis, single step, requirement of only one type of enzyme molecules (no co- polymer or cross linker), no harsh treatment of biologically hazardous solvents (like hydrofluoric acid in the case of SC-MS method[6]), environmentally friendly (utilized ionic liquid as reaction media), templated synthesis of platinum nanospheres, and functionality of phytase enzyme was retained. Based on above mentioned observations a simple plausible model is proposed and is depicted as scheme 2, to provide the interaction between phytase enzyme and hydrophilic IL and their role in reducing platinum ions and loading curcumin drug for its antitumor activity on cancer cells.

Self-assembled phytase nanospheres were formed in a polar Ionic Liquid [Bmim][BF$_4$] by structural reorganization of hydrophilic domains (catalytically-active) facing towards ionic
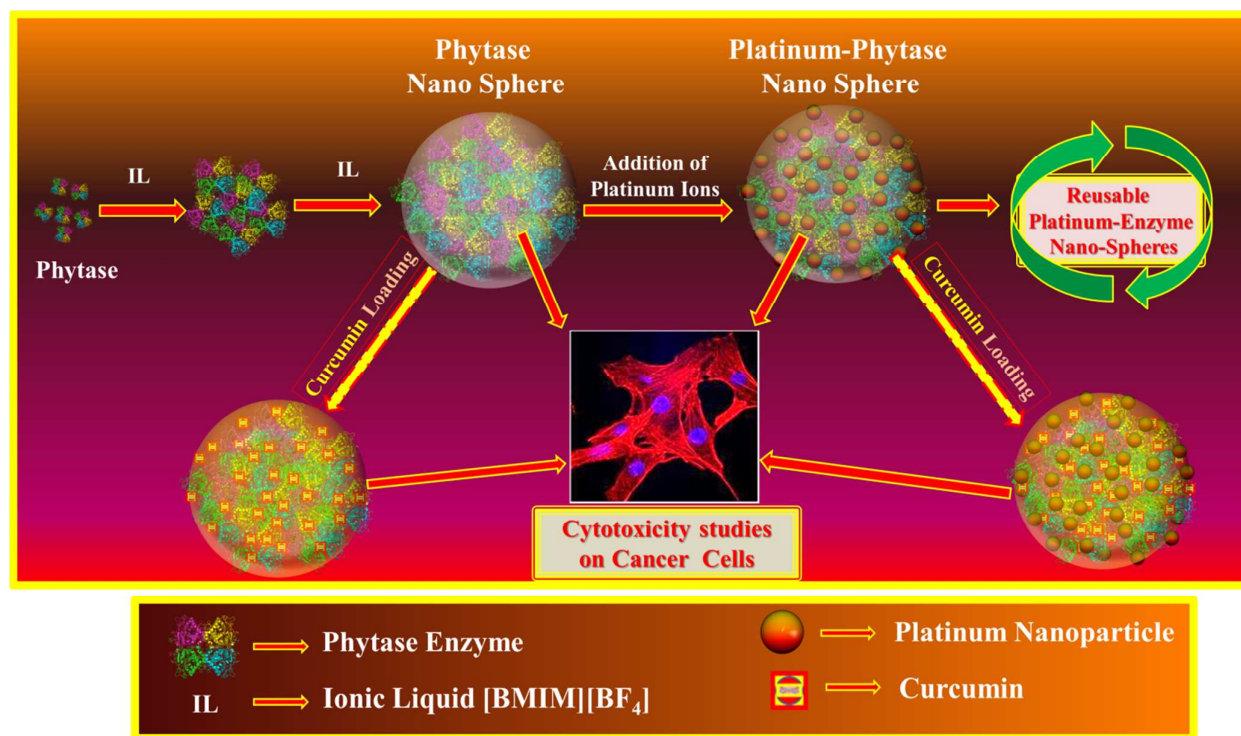
Scheme 2. Schematic illustration for self-assembly of phytase enzyme (*Aspergillus niger* phytase structure (http://www.ebi.ac.uk/pdbe/entry-images/1qfx_1600.png) taken from Protein data bank in Europe with due permission) in ionic liquid viz. [Bmim][BF$_4$], leading to phytase nanospheres, platinum-Phytase nanosphere. Curcumin was loaded on both these samples and entrapped in inner hydrophobic domains of protein template. All the samples were tested for their *in-vitro* anticancer activity and combinatorial effect on cancercells (cells shown here are only representative). Phytase encapsulated Platinum nanospheres were also tested for their enzyme reusability application and establish themselves as reusable enzyme nano-container.

liquid, while keeping their hydrophobic part interior like a micelle. Addition of platinum ions to the self-assembled phytase nanosphere forms a Pt-Phy nanosphere in [BMIM][BF$_4$]. Curcumin dissolved in oleic acid was further loaded into the self-assembled phytase nanospheres, and Pt-Phy nanospheres. Curcumin a hydrophobic drug tends to go inside the hydrophobic inner domains and /or molecular level voids of self-assembled Phytase nanospheres. Phytase, Phy-Curcumin, Pt-Phy and Pt-Phy-Curcumin were tested *in-vitro* for their anticancer activity on various tumor cells. Pt-Phy were also used for its enzyme reusability application and shown to be an excellent reusable, green enzyme nano-container.

Conclusions

In summary, we have shown in past that ionic liquids can be utilized as media for bio-macromolecular self-assembly at room temperature and it can result into hollow and solid silica spheres, and metal hollow spheres. The current work here to synthesize self-assembled enzyme nanospheres as a template for synthesizing platinum nanoparticles and nano-container to load curcumin drug expands the applicability of this system to utilize both inorganic and organic portion of hybrid nanosphere. Moreover this system shows promising application as an efficient drug delivery vehicle for tumor suppression. Higher concentration of drug in cancer cells can be potentially enhanced by amphiphilic biopolymer based drug delivery tools. Protein based nanoparticle could offer to reduce burden on current health care system by reducing the need for premedication and at the same time, the combinatorial drug delivery synergistically enhances the efficacy and efficiency of drugs and would accelerate killing of the tumor more efficiently than the respective combinations of drugs.

Combination of this sophisticated combination of various functionalities within a single nanosphere attracts the current tools to develop protein sphere as multifunctional bio-materials. After incorporating surface functionalization and biocompatibility, self-assembled protein spheres in ionic liquid can be considered as promising next generation drug delivery tool.

Acknowledgements

Notes and references

1. R. Duncan, *Nat Rev Drug Discov*, 2003, **2**, 347-360.
2. K. E. Uhrich, S. M. Cannizzaro, R. S. Langer and K. M. Shakesheff, *Chemical Reviews*, 1999, **99**, 3181-3198.
3. G. A. Hughes, *Nanomedicine: Nanotechnology, Biology and Medicine*, **1**, 22-30.
4. B. M. Discher, Y.-Y. Won, D. S. Ege, J. C. M. Lee, F. S. Bates, D. E. Discher and D. A. Hammer, *Science*, 1999, **284**, 1143-1146.
5. F. Caruso, R. A. Caruso and H. Möhwald, *Science*, 1998, **282**, 1111-1114.
6. Y. Wang, A. S. Angelatos and F. Caruso, *Chemistry of Materials*, 2007, **20**, 848-858.
7. L. Kang, B. G. Chung, R. Langer and A. Khademhosseini, *Drug Discovery Today*, 2008, **13**, 1-13.
8. C. S. Peyratout and L. Dähne, *Angewandte Chemie International Edition*, 2004, **43**, 3762-3783.
9. K. D. Hermanson, D. Huemmerich, T. Scheibel and A. R. Bausch, *Advanced Materials*, 2007, **19**, 1810-1815.
10. C. Wang, R. J. Stewart and J. KopeCek, *Nature*, 1999, **397**, 417-420.
11. G. Wang and H. Uludag, *Expert Opinion on Drug Delivery*, 2008, **5**, 499-515.
12. Y.-b. Lim, K.-S. Moon and M. Lee, *Angewandte Chemie International Edition*, 2009, **48**, 1601-1605.
13. G. D. Rose, P. J. Fleming, J. R. Banavar and A. Maritan, *Proceedings of the National Academy of Sciences*, 2006, **103**, 16623-16633.
14. D. Dimitrov, in *Therapeutic Proteins*, eds. V. Voynov and J. A. Caravella, Humana Press, 2012, vol. 899, pp. 1-26.
15. L. Zhang, L. Laug, W. Münchgesang, E. Pippel, U. Gösele, M. Brandsch and M. Knez, *Nano Letters*, 2009, **10**, 219-223.
16. M. E. Davis, Z. Chen and D. M. Shin, *Nat Rev Drug Discov*, 2008, **7**, 771-782.
17. W. Lohcharoenkal, L. Wang, Y. C. Chen and Y. Rojanasakul, *BioMed Research International*, 2014, **2014**, 12.
18. A. S. Lammel, X. Hu, S.-H. Park, D. L. Kaplan and T. R. Scheibel, *Biomaterials*, 2010, **31**, 4583-4591.
19. X. Pan, S. Yu, P. Yao and Z. Shao, *Journal of Colloid and Interface Science*, 2007, **316**, 405-412.
20. V. Mishra, S. Mahor, A. Rawat, P. N. Gupta, P. Dubey, K. Khatri and S. P. Vyas, *Journal of Drug Targeting*, 2006, **14**, 45-53.
21. F. Kratz, *Journal of Controlled Release*, 2008, **132**, 171-183.
22. T. L. Greaves and C. J. Drummond, *Chemical Society Reviews*, 2008, **37**, 1709-1726.
23. S. K. Soni, S. Sarkar, N. Mirzadeh, P. R. Selvakannan and S. K. Bhargava, *Langmuir*, 2015, **31**, 4722-4732.
24. Z. Ma, J. Yu and S. Dai, *Advanced Materials*, 2010, **22**, 261-285.
25. Y. Jiang, C. Guo, H. Xia, I. Mahmood, C. Liu and H. Liu, *Journal of Molecular Catalysis B: Enzymatic*, 2009, **58**, 103-109.
26. J.-Q. Lai, Z. Li, Y.-H. Lu and Z. Yang, *Green Chemistry*, 2011, **13**, 1860-1868.
27. N. Kimizuka and T. Nakashima, *Langmuir*, 2001, **17**, 6759-6761.
28. K. Bhavsar, P. Buddhiwant, S. K. Soni, D. Depan, S. Sarkar and J. M. Khire, *Process Biochemistry*, 2013, **48**, 1618-1625.
29. S. K. Soni, R. Ramanathan, P. J. Coloe, V. Bansal and S. K. Bhargava, *Langmuir*, 2010, **26**, 16020-16024.

RSC Advances Accepted Manuscript

ARTICLE

30. S. K. Soni, P. R. Selvakannan, S. K. Bhargava and V. Bansal, *Langmuir*, 2012, **28**, 10389-10397.
31. G. Walsh, *Nat Biotech*, 2010, **28**, 917-924.
32. S. K. Singh, *Journal of Pharmaceutical Sciences*, 2011, **100**, 354-387.
33. S. K. Soni, A. Magdum and J. M. Khire, *World J Microbiol Biotechnol*, 2010, **26**, 2009-2018.
34. Q. Zhao, W. Chen, Y. Chen, L. Zhang, J. Zhang and Z. Zhang, *Bioconjugate Chemistry*, 2011, **22**, 346-352.
35. S. Soni and J. Khire, *World J Microbiol Biotechnol*, 2007, **23**, 1585-1593.
36. J. K. Heinonen and R. J. Lahti, *Analytical Biochemistry*, 1981, **113**, 313-317.
37. S. Sarkar and D. Sarkar, *Journal of biomolecular screening*, 2012, **17**, 966-973.
38. P. R. Twentyman and M. Luscombe, *British Journal of Cancer*, 1987, **56**, 279-285.
39. A. H. J. Ullah, B. J. Cummins and H. C. Dischinger Jr, *Biochemical and Biophysical Research Communications*, 1991, **178**, 45-53.
40. S. Behrens, K. Rahn, W. Habicht, K. J. Böhm, H. Rösner, E. Dinjus and E. Unger, *Advanced Materials*, 2002, **14**, 1621-1625.
41. L. Yu, I. A. Banerjee and H. Matsui, *Journal of Materials Chemistry*, 2004, **14**, 739-743.
42. M.-T. Huang, Y.-R. Lou, W. Ma, H. L. Newmark, K. R. Reuhl and A. H. Conney, *Cancer Research*, 1994, **54**, 5841-5847.
43. R. K. Giri, V. Rajagopal and V. K. Kalra, *Journal of Neurochemistry*, 2004, **91**, 1199-1210.
44. D. N. Brindley and D. W. Waggoner, *Journal of Biological Chemistry*, 1998, **273**, 24281-24284.
45. D. W. Waggoner, A. Gómez-Muñoz, J. Dewald and D. N. Brindley, *Journal of Biological Chemistry*, 1996, **271**, 16506-16509.
46. G. Szakacs, J. K. Paterson, J. A. Ludwig, C. Booth-Genthe and M. M. Gottesman, *Nat Rev Drug Discov*, 2006, **5**, 219-234.
47. J. Jia, F. Zhu, X. Ma, Z. W. Cao, Y. X. Li and Y. Z. Chen, *Nat Rev Drug Discov*, 2009, **8**, 111-128.
48. J. L. Nitiss, *Nature reviews. Cancer*, 2009, **9**, 338-350.
49. L. Zhao, M. G. Wientjes and J. L. S. Au, *Clinical Cancer Research*, 2004, **10**, 7994-8004.
50. Y. Matsumura and H. Maeda, *Cancer Research*, 1986, **46**, 6387-6392.
51. C. J. F. Rijcken, O. Soga, W. E. Hennink and C. F. v. Nostrum, *Journal of Controlled Release*, 2007, **120**, 131-148.
52. H. R. Luckarift, J. C. Spain, R. R. Naik and M. O. Stone, *Nat Biotech*, 2004, **22**, 211-213.
53. A. Gutmanas, Y. Alhroub, G. M. Battle, J. M. Berrisford, E. Bochet, M. J. Conroy, J. M. Dana, M. A. Fernandez Montecelo, G. van Ginkel, S. P. Gore, P. Haslam, R. Hatherley, P. M. S. Hendrickx, M. Hirshberg, I. Lagerstedt, S. Mir, A. Mukhopadhyay, T. J. Oldfield, A. Patwardhan, L. Rinaldi, G. Sahni, E. Sanz-García, S. Sen, R. A. Slowley, S. Velankar, M. E. Wainwright and G. J. Kleywegt, *Nucleic Acids Research*, 2013.
54. D. Kostrewa, M. Wyss, A. D'Arcy and A. P. van Loon, *J Mol Biol*, 1999, **288**, 965-974.